Hybrid Logical-Physical Qubit Interaction for Quantum Metrology

Nadav Carmel* and Nadav Katz†
The Hebrew University of Jerusalem

(Dated: April 17, 2023)

We demonstrate a property of the quantum 5-qubit stabilizer code that enables the interaction between qubits of different logical layers, and conduct a full density-matrix simulation of an interaction between a logical and a physical qubit. We find under which circumstances it gives an advantage, changing the circuit depth and noise level with decoherence processes at play. Finally, we use our method to find the noise threshold for sensing a signal using quantum phase estimation procedures.

I. INTRODUCTION

In the field of quantum metrology, we are most interested in finding ways to recover the Heisenberg-limit scaling, promising that the error in estimating our observable scales as one over the number of measurements, probing time or number of probes [1]. Recent results indicate that this limit cannot be recovered in the presence of general Markovian noise if the Hamiltonian lies in the span of the noise operators.[2–6]. Much effort has been made to recover the Heisenberg-limit scaling using quantum error correction [1, 3, 4, 7–14]. All these efforts focus on sequential quantum metrology, encoding the sensor as a logical qubit and using sophisticated methods to correct the errors while not correcting the signal itself.

Degen *et al.* [15] defines quantitatively the Dynamic Range of a quantum sensor, and finds it scales as the square root of the measurement time. This is where algorithmic quantum sensing is important - it gives a way to enlarge the dynamic range of a quantum sensor to scale as the measurement time by giving an appropriate weighting to different quantum measurements, thus approaching the Heisenberg limit. Recently the use of algorithmic quantum sensing had caught the attention of the community [13, 16]. While most algorithmic sensing protocols are variations of the family of algorithms called Quantum Phase Estimation (QPE), QPE has numerous applications in other areas of study [17–21], the most famous one being Shor's algorithm. Thus a lot of study has been done on how QPE performs under the presence of noise [22–25]. This Heisenberg-limit scaling is achievable if the probability distribution is not biased, according to [5, 15]. But in the presence of decoherence the probability distribution attained from QPE algorithms is biased, making it impossible to achieve the Heisenberg-limit. In this work we give a way of making it less biased, thus approaching to the Heisenberg limit.

The existence of ancilla qubits in algorithmic quantum sensing protocols opens a new realm to study - performing error correction or error detection on the ancillas instead of on the sensor. Making only the ancilla logical while letting the sensor remain a physical sensor, enforces the need of hybrid logical-physical interaction. Although we could focus on making this interaction fault-tolerant [26] with flag fault-tolerance [27–31], for the purpose of quantum sensing we do not need the ability of computing endlessly - we only need a limited number of successful runs. Applying post selection on the sensor has proved to be a vital tool for any experimental implementation of sensing, and a number of works on the subject has been published in recent years [6, 25, 32–35]. It has been shown that the error in verified phase estimation [25], an error mitigation technique based on what we call sensor post-selection (SPS), scales as the squared probability for a single gate error p^2.

In this work, we take advantage of error propagation from the sensor qubit to the logical ancilla qubit. We get rid of a larger portion of the noise by encoding some of it on the redundant degrees of freedom of the Hilbert space of the logical ancilla, applying only error detection and post-selecting the results. We use the simple 5-qubit code. This code has a nice attribute: all errors with a weight smaller or equal to 2 cause a non-trivial syndrome. Thus if the probability of error in one ancilla qubit in the whole algorithm is p, then the probability of error after logically post-selecting (LPS) is proportional to p^3. See [36] for the 5-qubit-code stabilizers and a syndrome-cause table.

II. METHODS

Throughout the paper a fidelity between a 6-qubit-state and a 2-qubit-state has been calculated. This has been done by taking the 6-qubit-state's density matrix ρ and calculating the effective reduced density matrix ρ':

$$\rho' = \begin{pmatrix} \langle 0_L0|\rho|0_L0\rangle & \langle 0_L0|\rho|0_L1\rangle & \langle 0_L0|\rho|1_L0\rangle & \langle 0_L0|\rho|1_L0\rangle \\ \langle 0_L1|\rho|0_L0\rangle & \langle 0_L1|\rho|0_L1\rangle & \langle 0_L1|\rho|1_L0\rangle & \langle 0_L1|\rho|1_L0\rangle \\ \langle 1_L0|\rho|0_L0\rangle & \langle 1_L0|\rho|0_L1\rangle & \langle 1_L0|\rho|1_L0\rangle & \langle 1_L0|\rho|1_L0\rangle \\ \langle 1_L1|\rho|0_L0\rangle & \langle 1_L1|\rho|0_L1\rangle & \langle 1_L1|\rho|1_L0\rangle & \langle 1_L1|\rho|1_L0\rangle \end{pmatrix} \tag{1}$$

Note that this is not necessarily a pure state. Performing LPS in our simulation is done by projecting the state onto the code, forcing each stabilizer to measure '0', see

* nadav.carmel1@huji.mail.ac.il
† nadav.katz@mail.huji.ac.il

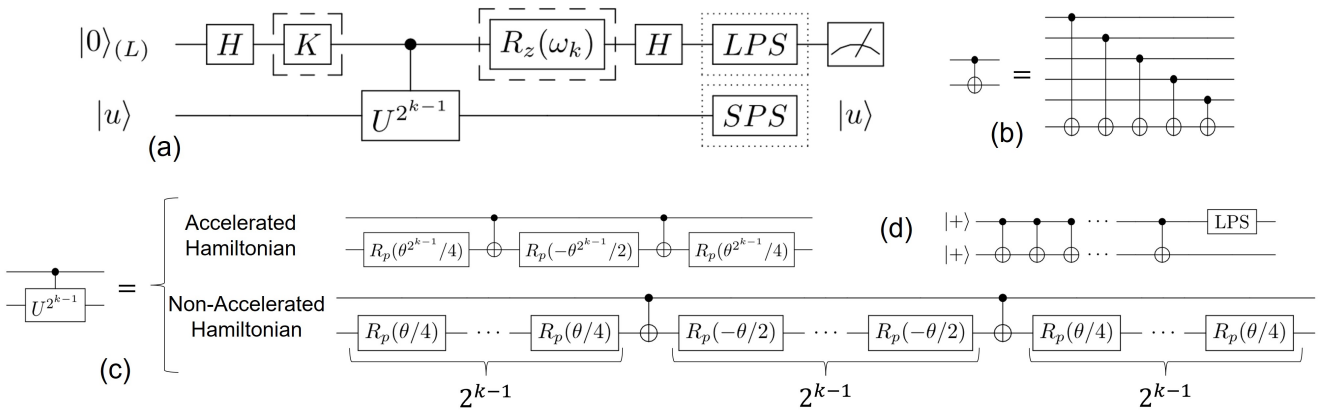

FIG. 1: Circuits used in this work. (a) Iterative versions of Quantum Phase Estimation. The dashed K gate appears only in Kitaev's iterative version, where K can be $K = S$ and $K = I$. The dashed R_z gate appears only in Iterative Phase Estimation Algorithm (IPEA), where the feedback angle depends on the previously measured bits through $\omega_k = -2\pi(0.0x_{k+1}x_{k+2}\ldots x_m)$, and $\omega_m = 0$.. The dotted LPS (Logical Post Selection) and SPS (Sensor Post Selection) gates appear in circuits as described in the main text and other figures. (b) Logically controlled CNOT gate, with the first 5 qubits acting as a logical qubit and the sixth qubit as the target qubit, encoded one logical layer lower then the control. (c) The controlled operation in this work is a single qubit rotation gate where $p = x$ or $p = z$. In the figure are implementations of accelerated and non-accelerated controlled signal Hamiltonians. (d) The circuit used for exploring logical-physical interaction length, Fig. 2.

[36] for additional details. In addition, when we perform error correction and the resulting state is not within the code, the reduction operation of Eq. 1 is not trace preserving. Due to the projective nature of these operations, to calculate the fidelity or distance between two states, where one of them is not a pure density matrix, we save the trace of each one and normalize them before hand.

A. Hybrid Entangling Gate and Logical Gates

Since any multi-qubit gate can be decomposed into single qubit gates and CNOT gates [37], our focus should be understanding how to implement the CNOT gate between logical and physical qubits, as control and target respectively. Some quantum error correction codes (QECC) have a useful parity attribute: The logical states, $|0\rangle_L$ and $|1\rangle_L$, are made up of a sum of quantum states with an even or odd number of 1's, respectively. One such code is the 5-qubit-code, with basis states defined in [36]. In the case of one logical layer, this attribute allows us to implement the CNOT gate in a semi-transversal manner, as in Fig. 1 (b). This can be generalized trivially for any number of logical layers, provided that the quantum code used for each layer has this attribute. All logical gates that are necessary for the QPE algorithm using the 5-qubit code are provided in the [36].

B. Quantum Phase Estimation

Quantum phase estimation is a family of algorithms. Suppose a unitary operator U has an eigenvector $|u\rangle$ with eigenvalue $e^{2\pi i\phi}$, where the value of ϕ is unknown. The goal of the phase estimation algorithm is to estimate ϕ. To perform the estimation, we assume we have available black boxes capable of preparing the state $|u\rangle$ and performing controlled-U^{2^j} operations for some positive integer j. The algorithm uses two quantum registers, one for the measured operator U and one for ancilla qubits needed for the computation. Phase estimation was first introduced by Kitaev [38]. In our study we use two iterative versions of the algorithm, both presented in Fig. 1 (1). The iterative versions use only one ancilla qubit to perform the phase estimation, and so they have great importance in the age of Noisy Intermediate Scale Quantum (NISQ) computers, since we cannot currently use many qubits simultaneously. We use Kitaev's approach to simulate the case of accelerated Hamiltonians, and IPEA to simulate the case of unaccelerated Hamiltonians. See the Supplemental Material for more information on these two iterative versions of the algorithm.

III. RESULTS

Throughout this work we separate two scenarios:

a. Target: Accuracy - In this scenario we give no consideration to the lost information. In the presence of decoherence, quantum phase estimation will converge (given an infinite amount of trials) to biased measure-

ment probabilities P_0, P_1 different from the ideal. In some cases we may be interested in getting this systematic error as low as possible, and we wouldn't care about how much information we have lost by post selecting. Algorithmic quantum sensing approaches the Heisenberg limit only for unbiased distributions, and using logical post selection allows us to make the distribution less biased, see Fig. 3 (a).

b. Resource: Minimal Number of Trials - In this scenario we consider the lost information in our calculations, in various ways - see Eq. 2 or [36]. In other, more common scenarios of quantum sensing, the lost information and number of trials does play a role, and a strong evidence for that is the fact that sensitivity is often defined per root Hertz. The thresholds obtained while considering the cost of post selection are depicted in Fig. 3 (b).

A. Exploring Logical-Physical Interaction Length

As mentioned earlier, each multi-qubit interaction can be reduced to single qubit gates and simple CNOT or CZ entangling gates. It is interesting to ask how does the threshold value (in which logical control is better then physical control) depend on the number of entangling gates? To answer this question, we take $T_1/T_g = \infty$ for all qubits, and a varying T_2/T_g for all qubits. We also take a varying number of CNOT gates, in the range [1,200), see Fig. 1 (d) for the simulated circuit. We start with the initial state $|++\rangle$ which is an eigenstate of the CNOT gate, and is a highly vulnerable state to T_2 noise. The first $|+\rangle$ in the tensor product may represent the logical qubit or a physical qubit. We apply N_g CNOT gates and then apply noisy LPS. We calculate and save the fidelity of the output state and $|++\rangle$, and plot a color map of the fidelity difference between the logical and the physical control (Fig. 2) where one axis is the number of entangling gates, and the second is the worst case single gate fidelity. Note that we apply noisy syndrome extraction, so the circuit depth has a constant overhead of approximately 20 gates. As we can see, there is a range of circuit depth and gate fidelities in which the logical control is better then the physical control. Here a give no consideration whatsoever to the lost information (the scenario is *Target: Accuracy*) but this feature is also observable in the non-accelerated Hamiltonian, *Resource: Minimal Number of Trials* scenario, as observed in Fig. 3 (b).

B. Kitaev's Approach with Accelerated Hamiltonians

Algorithmic quantum sensing using the quantum phase estimation algorithm is especially powerful under the assumption of accelerated Hamiltonians - having a black-box that can apply high powers of the time evolution operator with high fidelity. Accelerated Hamiltonians were studied in depth in the context of algorithmic complexity theory and super-resolution [39, 40]. This can be achieved via situation-specific methods like applying a sensed magnetic field in different angles, or by using general methods like QAQC [41], or VFF [42]. For our study we first assume accelerated Hamiltonians implemented as in Fig. 1 (c) and we simulate one iteration of Kitaev's approach (Fig. 1(a)), with logical post selection (LPS) and sensor post selection (SPS). We average over 10 angles uniformly distributed in the range $[0, 2\pi)$ and calculate (after post selection) the fidelity with the state of the two-qubit quantum register after an ideal run right before the measurement (and thus assume a perfect measurement). We do that for the physical ancilla approach, and for our approach with a logical ancilla qubit. The results are plotted in Fig. 3 (a), where we include the fidelity of the error-corrected state. Note that the error-corrected state shows a stochastic behaviour which was averaged in the figure, due to it's 'random' nature - a mistake in the syndrome extraction leads to the application of a faulty correction operator, and note that we have only one round of error correction in the circuit. Confirming the improved scaling of the error probability,

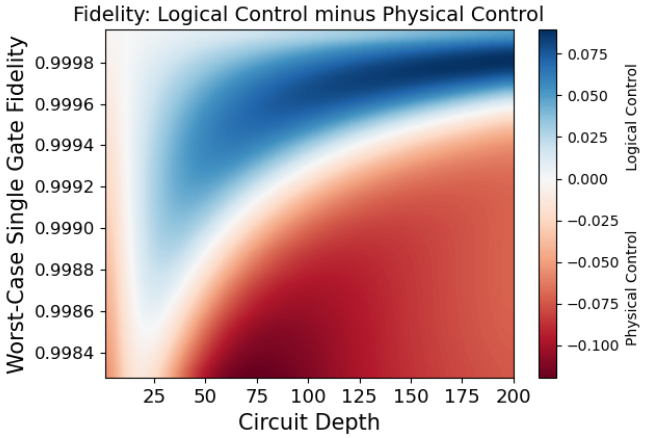

FIG. 2: Mapping the thresholds of logical and physical control for noise level and circuit depth, simulating the circuit in Fig. 1 (d). Here all qubits are noisy (susceptible only to dephasing) in all stages of the circuit, including syndrome extraction. The relevant scenario is *Target: Accuracy*. The white line is the location of the threshold, and blue/red areas are the fidelity difference at the end of the circuit. A non-monotonic behaviour of the fidelity with circuit depth is observed both in the above figure and in Fig. 3 (b). The values reached in this work are a result of specific simulation parameters and are expected to change with changes in quantum hardware, but the overall structure of the dependence is expected to stay similar.

TABLE I: Thresholds for Accelerated Hamiltonian from the data of Fig. 3 (a). The table shows worst-case single gate fidelity (WCSGF) and worst-case entangling gate fidelity (WCEGF), calculated by putting qubits in their most susceptible state to the applied noise - for example, the state $|+\rangle$ for dephasing and $|1\rangle$ for amplitude damping.

Circuit	T_2/T_g	WCSGF	WCEGF
$K = I$	24	0.99	0.98
$K = S$	40	0.994	0.987

and similar graphs giving complementary information, are available in [36].

Counter intuitively, we get a threshold for which logical control (green line) is better then physical control (blue line). This is counter intuitive because only the ancillas are noisy. Apparently, there are circumstances in which it is better to use five noisy ancillas then only one noisy ancilla. The thresholds are summarised in Table I. Surprisingly, these thresholds are well within the capabilities of today's [43] state of the art technology! Thus, for the purpose of accurate sensing, with infinite sensing time, using logical post selection is the better approach for the NISQ era. This is of course true only in scenarios in which we aim for accuracy over resources. In the resource limited scenario logical post selection only spoils the results due to the high percentage of information lost. The following part of our study will focus on finding the circumstances in which logical post selection is helpful even in the resource limited scenarios. For a discussion on resource limitation for sensing with accelerated Hamiltonian, see

C. Iterative Phase Estimation Algorithm without Accelerated Hamiltonains

Our previous results show no advantage of using logical control for quantum sensing with limited resources, but those results are the product of a highly non-trivial assumption - that we have access to accelerated Hamiltonians. Here give up on this assumption and use the IPEA (Fig.1 (a) with LPS and without SPS), which outputs a measured phase and a standard deviation in that phase. We pick the irrational phase $\phi = 2\pi/\sqrt{3}$ and evaluate it for up to nine binary digits of accuracy, requiring a maximum of around $3 * 2^8 \approx 760$ consecutive applications of gates. Thus the maximum circuit depth we use, including syndrome extraction, is around 800 gates, approximately 40 times longer then the accelerated case. We define the *lost information* to be $l_i = 1 - Tr(\rho')$ where ρ' is the reduced 2-qubit density matrix defined in Eq.1, and compare the standard deviation difference $(\sigma - \sigma_{ideal})\sqrt{N}$ for the physical and the logical ancilla approaches. The standard deviation is defined to be, in

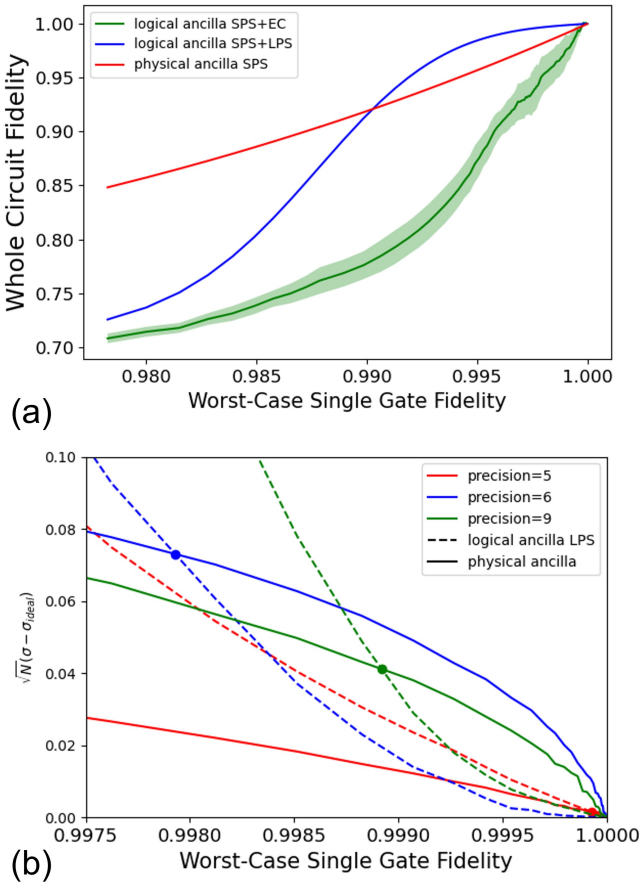

FIG. 3: (a) Fidelity after one iteration of Kitaev's iterative approach with accelerated sensing Hamiltonian averaged over 10 angles, measuring the operator $R_z(\theta)$ with sensor initialized in the ground state. The red line represents physical ancilla with SPS, the blue line logical ancilla with SPS and LPS while the green line is logical ancilla with error correction right before the measurement. Here the sensor is perfect and the ancillas are noisy, susceptible only to dephasing. The scenario is *Target: Accuracy*. These graphs are for $K = I$ and similar graphs are available for $K = S$ in [36]. It is clear that there is a threshold (table I) in which using LPS outputs a state closer to the ideal. (b) Error in estimating the phase of non-accelerated signal Hamiltonian $R_x(\frac{2\pi}{\sqrt{3}})$ with sensor initialized in the state $|+\rangle$, in comparison to the ideal, using IPEA. The relative error is plotted for desired precision of 5,6,9 digits, while continuous line represents physical ancilla and dashed line represents logical ancilla and LPS. Here the ancillas are perfect and the sensor is noisy, susceptible only to dephasing. The scenario is *Resource: Minimal Number of Trials*. It is clear that the threshold for which using LPS outputs a smaller error is dependent on the circuit depth. The non-monotonic nature of this phenomenon is demonstrated in Fig. 2.

general,

$$\sigma = \frac{\sigma'}{\sqrt{N(1-l_i)}} \tag{2}$$

Where σ' is the standard deviation of the histogram of phase results, N is the total number of trials. We expect to see the most significant improvement for the realistic case of a noisy sensor and good (perfect) ancillas. For this end we put the sensor in the eigenstate $|+\rangle$ and measure the operator $R_x(\frac{2\pi}{\sqrt{3}})$. We assume perfect ancillas and allow only dephasing to occur to the sensor. The results are plotted in Fig. 3 (b). A similar scenario, where the sensor is put in the excited state and is susceptible to T_1 noise, with perfect ancillas, measuring $R_z(\frac{2\pi}{\sqrt{3}})$. As a sanity check we also simulate a measurement of $R_z(\frac{2\pi}{\sqrt{3}})$ with sensor qubit initialized in the excited state $|1\rangle$, with noisy (dephasing) ancillas and perfect sensor. As expected, adding noisy ancillas to a perfect sensor does not improve the error in estimating the phase. The results of the above two scenarios are depicted in [36]. In the figure we see a second manifestation of the phenomenon observed in Fig. 2 - the existence of a unique parameter regime in which logical-physical interaction provides an advantage.

IV. DISCUSSION

We have introduced the concept of logical-physical qubit interaction and found a unique parameter regime where it is beneficial to use this kind of interaction, as a function of the circuit depth and the worst case single gate fidelity, under the presence of dephasing being the most significant cause of error [22, 44]. We have defined a number of settings describing real-world sensing scenarios and we have used our idea to show an improvement of up to two orders of magnitude for algorithmic quantum sensing, by encoding the noise into a bigger Hilbert space and post selecting the purified state. Although the gate fidelities needed for the method to contribute to Heisenberg-limit scaling are far beyond the reach of today's state-of-the-art technology, we have witnessed situations in which using logical post selection leads to more precise measurements - where the ancilla are much more resiliant to noise then the sensor, or where Hamiltonian fast-forwarding is possible. The concept of hybrid logical-physical interaction has a considerable depth for further research. We think the concepts of logical control and logical post selection can be efficient in a big number of algorithms and purposes, especially ones that require long-lived ancilla qubits like state distillation, error mitigation and algorithmic sensing [45–47]. The most significant drawback of the method is the lost information due to post selection, and recent studies show promise to discover a method of simulating without the need for post selection [48]. This idea opens a wide set of frontiers to be searched, like finding a way to implement a an entangling gate between a logical qubit and a physical qubit with minimum error or error propagation, possibly by using flag fault-tolerance [27–31]. We have defined an attribute of quantum error correction codes that enables this kind of interaction. What other attributes are there, and how do they project on the topology of the interaction or on the general structure of these QECC? Can it be implemented with today's most promising codes, the surface codes [49]? These are examples of questions to be asked around the concept of logical-physical qubit interaction.

[1] S. Zhou, C. L. Zou, and L. Jiang, Saturating the quantum Cramér-Rao bound using LOCC, Quantum Science and Technology **5**, 36 (2020), arXiv:1809.06017.

[2] S. Zhou, M. Zhang, J. Preskill, and L. Jiang, Achieving the Heisenberg limit in quantum metrology using quantum error correction (2018), arXiv:1706.02445.

[3] D. Layden and P. Cappellaro, Spatial noise filtering through error correction for quantum sensing, npj Quantum Information **4**, 10.1038/s41534-018-0082-2 (2018), arXiv:1708.06729.

[4] I. Rojkov, D. Layden, P. Cappellaro, J. Home, and F. Reiter, Bias in Error-Corrected Quantum Sensing, Physical Review Letters **128**, 1 (2022), arXiv:2101.05817.

[5] M.-c. Chen, Y. Li, R.-z. Liu, D. Wu, Z.-e. Su, X.-l. Wang, L. Li, N.-l. Liu, C.-y. Lu, and J.-w. Pan, Directly Measuring a Multiparticle Quantum Wave Function via Quantum Teleportation, **030402**, 1 (2021).

[6] Y. Matsuzaki and S. Benjamin, Magnetic-field sensing with quantum error detection under the effect of energy relaxation, Physical Review A **95**, 1 (2017), arXiv:1611.10264.

[7] P. Cappellaro, D. Layden, L. Jiang, S. Zhou, M. Zhang, and J. Preskill, Error-corrected quantum sensing, , 51 (2019).

[8] Z. Ma, P. Gokhale, T.-X. Zheng, S. Zhou, X. Yu, L. Jiang, P. Maurer, and F. T. Chong, Adaptive Circuit Learning for Quantum Metrology, (2020), arXiv:2010.08702.

[9] F. Reiter, A. S. Sørensen, P. Zoller, and C. A. Muschik, Dissipative quantum error correction and application to quantum sensing with trapped ions, Nature Communications **8**, 10.1038/s41467-017-01895-5 (2017).

[10] D. A. Herrera-Martí, T. Gefen, D. Aharonov, N. Katz, and A. Retzker, Quantum Error-Correction-Enhanced Magnetometer Overcoming the Limit Imposed by Relaxation 10.1103/PhysRevLett.115.200501 (2014), arXiv:1410.7556.

[11] G. Arrad, Y. Vinkler, D. Aharonov, and A. Retzker, Increasing sensing resolution with error correction 10.1103/PhysRevLett.112.150801 (2013), arXiv:1310.3016.

[12] T. Unden, P. Balasubramanian, D. Louzon, Y. Vinkler, M. B. Plenio, M. Markham, D. Twitchen, I. Lovchinsky, A. O. Sushkov, M. D. Lukin, A. Retzker, B. Naydenov, L. P. Mcguinness, and F. Jelezko, *Quantum metrology enhanced by repetitive quantum error correction*, Tech. Rep.

[13] T. Kapourniotis and A. Datta, Fault-tolerant quantum metrology, Physical Review A **100**, 10.1103/PhysRevA.100.022335 (2019), arXiv:1807.04267.

[14] Q. Zhuang, J. Preskill, and L. Jiang, Distributed quantum sensing enhanced by continuous-variable error correction, New Journal of Physics **22**, 1 (2020), arXiv:1910.14156.

[15] C. L. Degen, F. Reinhard, and P. Cappellaro, Quantum sensing 10.1103/RevModPhys.89.035002 (2016), arXiv:1611.02427.

[16] M. Takita, K. Inoue, S. Lekuch, Z. K. Minev, J. M. Chow, and J. M. Gambetta, Exploiting dynamic quantum circuits in a quantum algorithm with superconducting qubits, (2021), arXiv:arXiv:2102.01682v1.

[17] T. E. O'Brien, B. Tarasinski, and B. M. Terhal, Quantum phase estimation of multiple eigenvalues for small-scale (noisy) experiments 10.1088/1367-2630/aafb8e (2018), arXiv:1809.09697.

[18] P. M. Q. Cruz, G. Catarina, and R. Gautier, Optimizing quantum phase estimation for the simulation of Hamiltonian eigenstates, , 1 (2020), arXiv:arXiv:1910.06265v2.

[19] R. Santagati, J. Wang, A. A. Gentile, S. Paesani, N. Wiebe, J. R. Mcclean, P. J. Shadbolt, D. Bonneau, J. W. Silverstone, D. P. Tew, X. Zhou, and M. G. Thompson, Witnessing eigenstates for quantum simulation of Hamiltonian spectra, arXiv:arXiv:1611.03511v5.

[20] S. Kais, A Universal Quantum Circuit Scheme For Finding Complex Eigenvalues, arXiv:arXiv:1302.0579v5.

[21] J. Tilly, H. Chen, S. Cao, D. Picozzi, K. Setia, Y. Li, E. Grant, L. Wossnig, I. Rungger, G. H. Booth, and J. Tennyson, *The Variational Quantum Eigensolver: a review of methods and best practices*, Vol. 7394 (2021) pp. 0–1, arXiv:2111.05176.

[22] F. Chapeau-Blondeau and E. Belin, Fourier-transform quantum phase estimation with quantum phase noise, Signal Processing **170**, 1 (2020).

[23] M. Dobšíček, G. Johansson, V. Shumeiko, and G. Wendin, Arbitrary accuracy iterative quantum phase estimation algorithm using a single ancillary qubit: A two-qubit benchmark, Physical Review A - Atomic, Molecular, and Optical Physics **76**, 10.1103/PhysRevA.76.030306 (2007).

[24] I. Garc and D. L. Shepelyansky, Quantum phase estimation algorithm in presence of static imperfections, (2007), arXiv:arXiv:0711.1756v1.

[25] T. E. O'Brien, S. Polla, N. C. Rubin, W. J. Huggins, S. McArdle, S. Boixo, J. R. McClean, and R. Babbush, Error Mitigation via Verified Phase Estimation, PRX Quantum **2**, 1 (2021), arXiv:2010.02538.

[26] D. Aharonov, Fault-Tolerant Quantum Computation With Constant Error, , 1arXiv:9611025v2 [arXiv:quant-ph].

[27] R. Chao and B. W. Reichardt, Fault-tolerant quantum computation with few qubits 10.1038/s41534-018-0085-z (2017), arXiv:1705.05365.

[28] T. Tansuwannont, C. Chamberland, and D. Leung, *Flag fault-tolerant error correction, measurement, and quantum computation for cyclic CSS codes*, Tech. Rep., arXiv:1803.09758v3.

[29] R. Chao and B. W. Reichardt, Flag fault-tolerant error correction for any stabilizer code 10.1103/PRXQuantum.1.010302 (2019), arXiv:1912.09549.

[30] B. W. Reichardt, Fault-tolerant quantum error correction for Steane's seven-qubit color code with few or no extra qubits 10.1088/2058-9565/abc6f4 (2018), arXiv:1804.06995.

[31] D. M. Debroy and K. R. Brown, Extended flag gadgets for low-overhead circuit verification, Physical Review A **102**, 1 (2020), arXiv:2009.07752.

[32] B. M. Varbanov, F. Battistel, B. M. Tarasinski, V. P. Ostroukh, T. E. O'Brien, L. DiCarlo, and B. M. Terhal, Leakage detection for a transmon-based surface code, npj Quantum Information **6**, 1 (2020), arXiv:2002.07119.

[33] H. Kwon, C. Oh, Y. Lim, H. Jeong, and L. Jiang, Efficacy of virtual purification-based error mitigation on quantum metrology, , 1 (2023), arXiv:2303.15838.

[34] K. Yamamoto, S. Endo, H. Hakoshima, Y. Matsuzaki, and Y. Tokunaga, Error-Mitigated Quantum Metrology via Virtual Purification, Physical Review Letters **129**, 10.1103/PhysRevLett.129.250503 (2022), arXiv:2112.01850.

[35] D. R. Arvidsson-Shukur, N. Yunger Halpern, H. V. Lepage, A. A. Lasek, C. H. Barnes, and S. Lloyd, Quantum advantage in postselected metrology, Nature Communications **11**, 1 (2020), arXiv:1903.02563.

[36] See supplemental material at [url], .

[37] M. A. Nielsen and I. L. Chuang, *Quantum computation and quantum information* (Cambridge University Press, 2010) p. 676.

[38] A. Y. Kitaev, Quantum measurements and the Abelian Stabilizer Problem, , 1 (1995), arXiv:9511026 [quant-ph].

[39] Y. Atia and D. Aharonov, Fast-forwarding of Hamiltonians and exponentially precise measurements, Nature Communications **8**, 10.1038/s41467-017-01637-7 (2017), arXiv:1610.09619.

[40] Y. Aharonov and S. Popescu, *Measuring Energy, Estimating Hamiltonians, and the Time-Energy Uncertainty Relation*, Tech. Rep. (2002).

[41] S. Khatri, R. LaRose, A. Poremba, L. Cincio, A. T. Sornborger, and P. J. Coles, Quantum-assisted quantum compiling 10.22331/q-2019-05-13-140 (2018), arXiv:1807.00800.

[42] C. Cîrstoiu, Z. Holmes, J. Iosue, L. Cincio, P. J. Coles, and A. Sornborger, Variational fast forwarding for quantum simulation beyond the coherence time, npj Quantum Information **6**, 10.1038/s41534-020-00302-0 (2020), arXiv:1910.04292.

[43] A. Kandala, K. X. Wei, S. Srinivasan, E. Magesan, S. Carnevale, G. A. Keefe, D. Klaus, O. Dial, and D. C. McKay, Demonstration of a High-Fidelity CNOT for Fixed-Frequency Transmons with Engineered ZZ Suppression, (2020), arXiv:2011.07050.

[44] A. Yu and A. Y. Chernyavskiy, Proceedings of spie 10.1117/12.2522383 (2021).

[45] P. Czarnik, A. Arrasmith, L. Cincio, and P. J. Coles, Qubit-efficient exponential suppression of errors, arXiv:arXiv:2102.06056v2.

[46] C. Piveteau, D. Sutter, S. Bravyi, J. M. Gambetta, and K. Temme, Error mitigation for universal gates on encoded qubits, , 1arXiv:arXiv:2103.04915v1.

[47] W. J. Huggins, S. McArdle, T. E. O'Brien, J. Lee, N. C. Rubin, S. Boixo, K. B. Whaley, R. Babbush,

and J. R. McClean, Virtual Distillation for Quantum Error Mitigation, Physical Review X **11**, 41036 (2021), arXiv:2011.07064.

[48] M. Ippoliti and V. Khemani, Postselection-Free Entanglement Dynamics via Spacetime Duality, Physical Review Letters **126**, 60501 (2021), arXiv:2010.15840.

[49] E. Dennis, A. Kitaev, A. Landahl, and J. Preskill, Topological quantum memory, Journal of Mathematical Physics **43**, 4452 (2002), arXiv:0110143 [quant-ph].

[50] D. A. Steck, Quantum and Atom Optics, Lecture Notes, , 843 (2012).

[51] S. Johnstun and J.-F. Van Huele, Optimizing the Phase Estimation Algorithm Applied to the Quantum Simulation of Heisenberg-Type Hamiltonians, (2021), arXiv:2105.05018.

[52] T. J. Yoder, R. Takagi, and I. L. Chuang, Universal fault-tolerant gates on concatenated stabilizer codes, Physical Review X **6**, 10.1103/PhysRevX.6.031039 (2016), arXiv:1603.03948.

[53] H. Ahmadi and C.-F. Chiang, Quantum Phase Estimation with Arbitrary Constant-precision Phase Shift Operators, (2010), arXiv:1012.4727.

[54] S. Cheng, C. Cao, C. Zhang, Y. Liu, S.-Y. Hou, P. Xu, and B. Zeng, Simulating Noisy Quantum Circuits with Matrix Product Density Operators 10.1103/PhysRevResearch.3.023005 (2020), arXiv:2004.02388.